

Inclusive Double-Pomeron Exchange at the Fermilab Tevatron $\bar{p}p$ Collider

D. Acosta,¹⁴ T. Affolder,⁷ H. Akimoto,⁵¹ M. G. Albrow,¹³ D. Ambrose,³⁷ D. Amidei,²⁸ K. Anikeev,²⁷ J. Antos,¹ G. Apollinari,¹³ T. Arisawa,⁵¹ A. Artikov,¹¹ T. Asakawa,⁴⁹ W. Ashmanskas,² F. Afzar,³⁵ P. Azzi-Bacchetta,³⁶ N. Bacchetta,³⁶ H. Bachacou,²⁵ W. Badgett,¹³ S. Bailey,¹⁸ P. de Barbaro,⁴¹ A. Barbaro-Galtieri,²⁵ V. E. Barnes,⁴⁰ B. A. Barnett,²¹ S. Baroiant,⁵ M. Barone,¹⁵ G. Bauer,²⁷ F. Bedeschi,³⁸ S. Behari,²¹ S. Belforte,⁴⁸ W. H. Bell,¹⁷ G. Bellettini,³⁸ J. Bellinger,⁵² D. Benjamin,¹² J. Bensinger,⁴ A. Beretvas,¹³ J. Berryhill,¹⁰ A. Bhatti,⁴² M. Binkley,¹³ D. Bisello,³⁶ M. Bishai,¹³ R. E. Blair,² C. Blocker,⁴ K. Bloom,²⁸ B. Blumenfeld,²¹ S. R. Blusk,⁴¹ A. Bocci,⁴² A. Bodek,⁴¹ G. Bolla,⁴⁰ A. Bolshov,²⁷ Y. Bonushkin,⁶ D. Bortoletto,⁴⁰ J. Boudreau,³⁹ A. Brandl,³¹ C. Bromberg,²⁹ M. Brozovic,¹² E. Brubaker,²⁵ N. Bruner,³¹ J. Budagov,¹¹ H. S. Budd,⁴¹ K. Burkett,¹⁸ G. Busetto,³⁶ K. L. Byrum,² S. Cabrera,¹² P. Calafiura,²⁵ M. Campbell,²⁸ W. Carithers,²⁵ J. Carlson,²⁸ D. Carlsmith,⁵² W. Caskey,⁵ A. Castro,³ D. Cauz,⁴⁸ A. Cerri,²⁵ L. Cerrito,²⁰ A. W. Chan,¹ P. S. Chang,¹ P. T. Chang,¹ J. Chapman,²⁸ C. Chen,³⁷ Y. C. Chen,¹ M.-T. Cheng,¹ M. Chertok,⁵ G. Chiarelli,³⁸ I. Chirikov-Zorin,¹¹ G. Chlachidze,¹¹ F. Chlebana,¹³ L. Christofek,²⁰ M. L. Chu,¹ J. Y. Chung,³³ W.-H. Chung,⁵² Y. S. Chung,⁴¹ C. I. Ciobanu,³³ A. G. Clark,¹⁶ M. Coca,⁴¹ A. Connolly,²⁵ M. Convery,⁴² J. Conway,⁴⁴ M. Cordelli,¹⁵ J. Cranshaw,⁴⁶ R. Culbertson,¹³ D. Dagenhart,⁴ S. D'Auria,¹⁷ S. De Cecco,⁴³ F. DeJongh,¹³ S. Dell'Agnello,¹⁵ M. Dell'Orso,³⁸ S. Demers,⁴¹ L. Demortier,⁴² M. Deninno,³ D. De Pedis,⁴³ P. F. Derwent,¹³ T. Devlin,⁴⁴ C. Dionisi,⁴³ J. R. Dittmann,¹³ A. Dominguez,²⁵ S. Donati,³⁸ M. D'Onofrio,³⁸ T. Dorigo,³⁶ N. Eddy,²⁰ K. Einsweiler,²⁵ E. Engels, Jr.,³⁹ R. Erbacher,¹³ D. Errede,²⁰ S. Errede,²⁰ R. Eusebi,⁴¹ Q. Fan,⁴¹ S. Farrington,¹⁷ R. G. Feild,⁵³ J. P. Fernandez,⁴⁰ C. Ferretti,²⁸ R. D. Field,¹⁴ I. Fiori,³ B. Flaughner,¹³ L. R. Flores-Castillo,³⁹ G. W. Foster,¹³ M. Franklin,¹⁸ J. Freeman,¹³ J. Friedman,²⁷ Y. Fukui,²³ I. Furic,²⁷ S. Galeotti,³⁸ A. Gallas,³² M. Gallinaro,⁴² T. Gao,³⁷ M. Garcia-Sciveres,²⁵ A. F. Garfinkel,⁴⁰ P. Gatti,³⁶ C. Gay,⁵³ D. W. Gerdes,²⁸ E. Gerstein,⁹ S. Giagu,⁴³ P. Giannetti,³⁸ K. Giolo,⁴⁰ M. Giordani,⁵ P. Giromini,¹⁵ V. Glagolev,¹¹ D. Glenzinski,¹³ M. Gold,³¹ N. Goldschmidt,²⁸ J. Goldstein,¹³ G. Gomez,⁸ M. Goncharov,⁴⁵ I. Gorelov,³¹ A. T. Goshaw,¹² Y. Gotra,³⁹ K. Goulianos,⁴² C. Green,⁴⁰ A. Gresele,³ G. Grim,⁵ C. Grosso-Pilcher,¹⁰ M. Guenther,⁴⁰ G. Guillian,²⁸ J. Guimaraes da Costa,¹⁸ R. M. Haas,¹⁴ C. Haber,²⁵ S. R. Hahn,¹³ E. Halkiadakis,⁴¹ C. Hall,¹⁸ T. Handa,¹⁹ R. Handler,⁵² F. Happacher,¹⁵ K. Hara,⁴⁹ A. D. Hardman,⁴⁰ R. M. Harris,¹³ F. Hartmann,²² K. Hatakeyama,⁴² J. Hauser,⁶ J. Heinrich,³⁷ A. Heiss,²² M. Hennecke,²² M. Herndon,²¹ C. Hill,⁷ A. Hocker,⁴¹ K. D. Hoffman,¹⁰ R. Hollebeck,³⁷ L. Holloway,²⁰ S. Hou,¹ B. T. Huffman,³⁵ R. Hughes,³³ J. Huston,²⁹ J. Huth,¹⁸ H. Ikeda,⁴⁹ C. Issever,⁷ J. Incandela,⁷ G. Introzzi,³⁸ M. Iori,⁴³ A. Ivanov,⁴¹ J. Iwai,⁵¹ Y. Iwata,¹⁹ B. Iyutin,²⁷ E. James,²⁸ M. Jones,³⁷ U. Joshi,¹³ H. Kambara,¹⁶ T. Kamon,⁴⁵ T. Kaneko,⁴⁹ J. Kang,²⁸ M. Karagoz Unel,³² K. Karr,⁵⁰ S. Kartal,¹³ H. Kasha,⁵³ Y. Kato,³⁴ T. A. Keaffaber,⁴⁰ K. Kelley,²⁷ M. Kelly,²⁸ R. D. Kennedy,¹³ R. Kephart,¹³ D. Khazins,¹² T. Kikuchi,⁴⁹ B. Kilminster,⁴¹ B. J. Kim,²⁴ D. H. Kim,²⁴ H. S. Kim,²⁰ M. J. Kim,⁹ S. B. Kim,²⁴ S. H. Kim,⁴⁹ T. H. Kim,²⁷ Y. K. Kim,²⁵ M. Kirby,¹² M. Kirk,⁴ L. Kirsch,⁴ S. Klimenko,¹⁴ P. Koehn,³³ K. Kondo,⁵¹ J. Konigsberg,¹⁴ A. Korn,²⁷ A. Korytov,¹⁴ K. Kotelnikov,³⁰ E. Kovacs,² J. Kroll,³⁷ M. Kruse,¹² V. Krutelyov,⁴⁵ S. E. Kuhlmann,² K. Kurino,¹⁹ T. Kuwabara,⁴⁹ N. Kuznetsova,¹³ A. T. Laasanen,⁴⁰ N. Lai,¹⁰ S. Lami,⁴² S. Lammel,¹³ J. Lancaster,¹² K. Lannon,²⁰ M. Lancaster,²⁶ R. Lander,⁵ A. Lath,⁴⁴ G. Latino,³¹ T. LeCompte,² Y. Le,²¹ J. Lee,⁴¹ S. W. Lee,⁴⁵ N. Leonardo,²⁷ S. Leone,³⁸ J. D. Lewis,¹³ K. Li,⁵³ C. S. Lin,¹³ M. Lindgren,⁶ T. M. Liss,²⁰ J. B. Liu,⁴¹ T. Liu,¹³ Y. C. Liu,¹ D. O. Litvintsev,¹³ O. Lobban,⁴⁶ N. S. Lockyer,³⁷ A. Loginov,³⁰ J. Loken,³⁵ M. Loreti,³⁶ D. Lucchesi,³⁶ P. Lukens,¹³ S. Lusin,⁵² L. Lyons,³⁵ J. Lys,²⁵ R. Madrak,¹⁸ K. Maeshima,¹³ P. Maksimovic,²¹ L. Malferrari,³ M. Mangano,³⁸ G. Manca,³⁵ M. Mariotti,³⁶ G. Martignon,³⁶ M. Martin,²¹ A. Martin,⁵³ V. Martin,³² M. Martínez,¹³ J. A. J. Matthews,³¹ P. Mazzanti,³ K. S. McFarland,⁴¹ P. McIntyre,⁴⁵ M. Menguzzato,³⁶ A. Menzione,³⁸ P. Merkel,¹³ C. Mesropian,⁴² A. Meyer,¹³ T. Miao,¹³ R. Miller,²⁹ J. S. Miller,²⁸ H. Minato,⁴⁹ S. Miscetti,¹⁵ M. Mishina,²³ G. Mitselmakher,¹⁴ Y. Miyazaki,³⁴ N. Moggi,³ E. Moore,³¹ R. Moore,²⁸ Y. Morita,²³ T. Moulik,⁴⁰ M. Mulhearn,²⁷ A. Mukherjee,¹³ T. Muller,²² A. Munar,³⁸ P. Murat,¹³ S. Murgia,²⁹ J. Nachtman,⁶ V. Nagaslaev,⁴⁶ S. Nahn,⁵³ H. Nakada,⁴⁹ I. Nakano,¹⁹ R. Naporra,²¹ F. Niell,²⁸ C. Nelson,¹³ T. Nelson,¹³ C. Neu,³³ M. S. Neubauer,²⁷ D. Neuberger,²² C. Newman-Holmes,¹³ C.-Y. P. Ngan,²⁷ T. Nigmanov,³⁹ H. Niu,⁴ L. Nodulman,² A. Nomerotski,¹⁴ S. H. Oh,¹² Y. D. Oh,²⁴ T. Ohmoto,¹⁹ T. Ohsugi,¹⁹ R. Oishi,⁴⁹ T. Okusawa,³⁴ J. Olsen,⁵² W. Orejudos,²⁵ C. Pagliarone,³⁸ F. Palmonari,³⁸ R. Paoletti,³⁸ V. Papadimitriou,⁴⁶ D. Partos,⁴ J. Patrick,¹³ G. Pauletta,⁴⁸ M. Paulini,⁹ T. Pauly,³⁵ C. Paus,²⁷ D. Pellett,⁵ A. Penzo,⁴⁸ L. Pescara,³⁶ T. J. Phillips,¹² G. Piacentino,³⁸ J. Piedra,⁸ K. T. Pitts,²⁰ A. Pompoš,⁴⁰ L. Pondrom,⁵² G. Pope,³⁹ T. Pratt,³⁵ F. Prokoshin,¹¹ J. Proudfoot,² F. Ptohos,¹⁵ O. Pukhov,¹¹ G. Punzi,³⁸ J. Rademacker,³⁵ A. Rakitine,²⁷ F. Ratnikov,⁴⁴ H. Ray,²⁸ D. Reher,²⁵ A. Reichold,³⁵ P. Renton,³⁵ M. Rescigno,⁴³ A. Ribon,³⁶ W. Riegler,¹⁸ F. Rimondi,³

L. Ristori,³⁸ M. Rivelino,⁴⁷ W. J. Robertson,¹² T. Rodrigo,⁸ S. Rolli,⁵⁰ L. Rosenson,²⁷ R. Roser,¹³ R. Rossin,³⁶ C. Rott,⁴⁰ A. Roy,⁴⁰ A. Ruiz,⁸ D. Ryan,⁵⁰ A. Safonov,⁵ R. St. Denis,¹⁷ W. K. Sakumoto,⁴¹ D. Saltzberg,⁶ C. Sanchez,³³ A. Sansoni,¹⁵ L. Santi,⁴⁸ S. Sarkar,⁴³ H. Sato,⁴⁹ P. Savard,⁴⁷ A. Savoy-Navarro,¹³ P. Schlabach,¹³ E. E. Schmidt,¹³ M. P. Schmidt,⁵³ M. Schmitt,³² L. Scodellaro,³⁶ A. Scott,⁶ A. Scribano,³⁸ A. Sedov,⁴⁰ S. Seidel,³¹ Y. Seiya,⁴⁹ A. Semenov,¹¹ F. Semeria,³ T. Shah,²⁷ M. D. Shapiro,²⁵ P. F. Shepard,³⁹ T. Shibayama,⁴⁹ M. Shimojima,⁴⁹ M. Shochet,¹⁰ A. Sidoti,³⁶ J. Siegrist,²⁵ A. Sill,⁴⁶ P. Sinervo,⁴⁷ P. Singh,²⁰ A. J. Slaughter,⁵³ K. Sliwa,⁵⁰ F. D. Snider,¹³ R. Snihur,²⁶ A. Solodsky,⁴² T. Speer,¹⁶ M. Spezziga,⁴⁶ P. Spicas,²⁷ F. Spinella,³⁸ M. Spiropulu,¹⁰ L. Spiegel,¹³ J. Steele,⁵² A. Stefanini,³⁸ J. Strogas,²⁰ F. Strumia,¹⁶ D. Stuart,⁷ A. Sukhanov,¹⁴ K. Sumorok,²⁷ T. Suzuki,⁴⁹ T. Takano,³⁴ R. Takashima,¹⁹ K. Takikawa,⁴⁹ P. Tamburello,¹² M. Tanaka,⁴⁹ B. Tannenbaum,⁶ M. Tecchio,²⁸ R. J. Tesarek,¹³ P. K. Teng,¹ K. Terashi,⁴² S. Tether,²⁷ J. Thom,¹³ A. S. Thompson,¹⁷ E. Thomson,³³ R. Thurman-Keup,² P. Tipton,⁴¹ S. Tkaczyk,¹³ D. Toback,⁴⁵ K. Tollefson,²⁹ D. Tonelli,³⁸ M. Tonnesmann,²⁹ H. Toyoda,³⁴ W. Trischuk,⁴⁷ J. F. de Troconiz,¹⁸ J. Tseng,²⁷ D. Tsybychev,¹⁴ N. Turini,³⁸ F. Ukegawa,⁴⁹ T. Unverhau,¹⁷ T. Vaiciulis,⁴¹ A. Varganov,²⁸ E. Vataga,³⁸ S. Vejcik III,¹³ G. Velev,¹³ G. Veramendi,²⁵ R. Vidal,¹³ I. Vila,⁸ R. Vilar,⁸ I. Volobouev,²⁵ M. von der Mey,⁶ D. Vucinic,²⁷ R. G. Wagner,² R. L. Wagner,¹³ W. Wagner,²² Z. Wan,⁴⁴ C. Wang,¹² M. J. Wang,¹ S. M. Wang,¹⁴ B. Ward,¹⁷ S. Waschke,¹⁷ T. Watanabe,⁴⁹ D. Waters,²⁶ T. Watts,⁴⁴ M. Weber,²⁵ H. Wenzel,²² W. C. Wester III,¹³ B. Whitehouse,⁵⁰ A. B. Wicklund,² E. Wicklund,¹³ T. Wilkes,⁵ H. H. Williams,³⁷ P. Wilson,¹³ B. L. Winer,³³ D. Winn,²⁸ S. Wolbers,¹³ D. Wolinski,²⁸ J. Wolinski,²⁹ S. Wolinski,²⁸ M. Wolter,⁵⁰ S. Worm,⁴⁴ X. Wu,¹⁶ F. Würthwein,²⁷ J. Wyss,³⁸ U. K. Yang,¹⁰ W. Yao,²⁵ G. P. Yeh,¹³ P. Yeh,¹ K. Yi,²¹ J. Yoh,¹³ C. Yosef,²⁹ T. Yoshida,³⁴ I. Yu,²⁴ S. Yu,³⁷ Z. Yu,⁵³ J. C. Yun,¹³ L. Zanello,⁴³ A. Zanetti,⁴⁸ F. Zetti,²⁵ and S. Zucchelli³¹

(CDF Collaboration)

¹*Institute of Physics, Academia Sinica, Taipei, Taiwan 11529, Republic of China*²*Argonne National Laboratory, Argonne, Illinois 60439, USA*³*Istituto Nazionale di Fisica Nucleare, University of Bologna, I-40127 Bologna, Italy*⁴*Brandeis University, Waltham, Massachusetts 02254, USA*⁵*University of California at Davis, Davis, California 95616, USA*⁶*University of California at Los Angeles, Los Angeles, California 90024, USA*⁷*University of California at Santa Barbara, Santa Barbara, California 93106, USA*⁸*Instituto de Fisica de Cantabria, CSIC-University of Cantabria, 39005 Santander, Spain*⁹*Carnegie Mellon University, Pittsburgh, Pennsylvania 15213, USA*¹⁰*Enrico Fermi Institute, University of Chicago, Chicago, Illinois 60637, USA*¹¹*Joint Institute for Nuclear Research, RU-141980 Dubna, Russia*¹²*Duke University, Durham, North Carolina 27708, USA*¹³*Fermi National Accelerator Laboratory, Batavia, Illinois 60510, USA*¹⁴*University of Florida, Gainesville, Florida 32611, USA*¹⁵*Laboratori Nazionali di Frascati, Istituto Nazionale di Fisica Nucleare, I-00044 Frascati, Italy*¹⁶*University of Geneva, CH-1211 Geneva 4, Switzerland*¹⁷*Glasgow University, Glasgow G12 8QQ, United Kingdom*¹⁸*Harvard University, Cambridge, Massachusetts 02138, USA*¹⁹*Hiroshima University, Higashi-Hiroshima 724, Japan*²⁰*University of Illinois, Urbana, Illinois 61801, USA*²¹*The Johns Hopkins University, Baltimore, Maryland 21218, USA*²²*Institut für Experimentelle Kernphysik, Universität Karlsruhe, 76128 Karlsruhe, Germany*²³*High Energy Accelerator Research Organization (KEK), Tsukuba, Ibaraki 305, Japan*²⁴*Center for High Energy Physics, Kyungpook National University, Taegu 702-701, Korea; Seoul National University, Seoul 151-742, Korea; and SungKyunKwan University, Suwon 440-746, Korea*²⁵*Ernest Orlando Lawrence Berkeley National Laboratory, Berkeley, California 94720, USA*²⁶*University College London, London WC1E 6BT, United Kingdom*²⁷*Massachusetts Institute of Technology, Cambridge, Massachusetts 02139, USA*²⁸*University of Michigan, Ann Arbor, Michigan 48109, USA*²⁹*Michigan State University, East Lansing, Michigan 48824, USA*³⁰*Institution for Theoretical and Experimental Physics, ITEP, Moscow 117259, Russia*³¹*University of New Mexico, Albuquerque, New Mexico 87131, USA*³²*Northwestern University, Evanston, Illinois 60208, USA*³³*The Ohio State University, Columbus, Ohio 43210, USA*³⁴*Osaka City University, Osaka 588, Japan*³⁵*University of Oxford, Oxford OX1 3RH, United Kingdom*

- ³⁶*Universita di Padova, Istituto Nazionale di Fisica Nucleare, Sezione di Padova, I-35131 Padova, Italy*
³⁷*University of Pennsylvania, Philadelphia, Pennsylvania 19104, USA*
³⁸*Istituto Nazionale di Fisica Nucleare, University and Scuola Normale Superiore of Pisa, I-56100 Pisa, Italy*
³⁹*University of Pittsburgh, Pittsburgh, Pennsylvania 15260, USA*
⁴⁰*Purdue University, West Lafayette, Indiana 47907, USA*
⁴¹*University of Rochester, Rochester, New York 14627, USA*
⁴²*Rockefeller University, New York, New York 10021, USA*
⁴³*Istituto Nazionale de Fisica Nucleare, Sezione di Roma, University di Roma I, "La Sapienza," I-00185 Roma, Italy*
⁴⁴*Rutgers University, Piscataway, New Jersey 08855, USA*
⁴⁵*Texas A&M University, College Station, Texas 77843, USA*
⁴⁶*Texas Tech University, Lubbock, Texas 79409, USA*
⁴⁷*Institute of Particle Physics, University of Toronto, Toronto M5S 1A7, Canada*
⁴⁸*Istituto Nazionale di Fisica Nucleare, University of Trieste, Udine, Italy*
⁴⁹*University of Tsukuba, Tsukuba, Ibaraki 305, Japan*
⁵⁰*Tufts University, Medford, Massachusetts 02155, USA*
⁵¹*Waseda University, Tokyo 169, Japan*
⁵²*University of Wisconsin, Madison, Wisconsin 53706, USA*
⁵³*Yale University, New Haven, Connecticut 06520, USA*
(Received 5 November 2003; published 28 September 2004)

We report results from a study of events with a double-Pomeron exchange topology produced in $\bar{p}p$ collisions at $\sqrt{s} = 1800$ GeV. The events are characterized by a leading antiproton and a large rapidity gap on the outgoing proton side. We find that the differential production cross section agrees in shape with predictions based on Regge theory and factorization, and that the ratio of double-Pomeron exchange to single diffractive production rates is relatively unsuppressed as compared to the $\mathcal{O}(10)$ suppression factor previously measured in single diffractive production.

DOI: 10.1103/PhysRevLett.93.141601

PACS numbers: 11.55.Jy, 12.40.Nn

The success of perturbative quantum chromodynamics (QCD) in describing strong interactions at high transverse momentum transfers rests on the factorization theorem, which allows hadronic cross sections to be expressed in terms of parton-level cross sections (hard scattering) convoluted with uniquely defined hadron parton densities. It is therefore not surprising that the breakdown of factorization we reported in a previous paper for dijet production [1], a process containing both a hard scattering and the characteristic rapidity gap signature of diffraction, has attracted considerable theoretical attention. Rapidity gaps, defined as regions of pseudorapidity [2] devoid of particles, are presumed to be formed in diffractive events by the exchange of Pomerons (\mathbb{P}), which in QCD correspond to entities of gluons and/or quarks with the quantum numbers of the vacuum [3] (see Fig. 1). The breakdown of factorization in diffraction is expressed as a suppression of the cross section and is generally attributed to additional partonic interactions within a diffractive event that spoil the rapidity gap signature [4,5]. In processes with two rapidity gaps, as in that with two forward gaps traditionally referred to as double-Pomeron exchange (DPE), shown in Fig. 1(b), it has been proposed that either both gaps survive or are simultaneously spoiled, leading to a largely unsuppressed ratio of two-gap to one-gap rates [6]. Such a scenario could explain our finding that the ratio of the rates of DPE to single diffractive (SD) dijet production is about 5

times larger than that of SD to nondiffractive (ND) dijet production [7].

Since rapidity gap formation is a nonperturbative phenomenon, soft (low transverse momentum) diffractive cross sections would be expected to exhibit a similar behavior. Indeed, the SD $\bar{p}p$ cross section has been found to be suppressed at high energies by a factor of ~ 10 relative to extrapolations from lower energy data based on Regge theory and factorization [8–10]. In this Letter, we present a measurement of the ratio of the inclusive DPE to SD cross sections in $\bar{p}p$ collisions at $\sqrt{s} = 1800$ GeV and compare our results with previous measurements [11] and with predictions from Regge theory

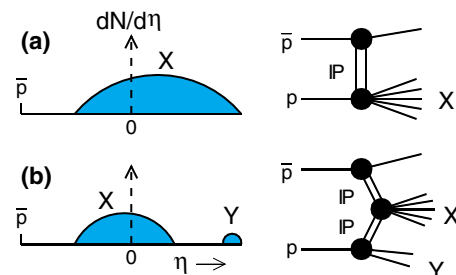


FIG. 1 (color online). Schematic diagrams and event topologies for (a) single diffraction, $\bar{p} + p \rightarrow \bar{p} + X$, and (b) double-Pomeron (\mathbb{P}) exchange, $\bar{p} + p \rightarrow \bar{p} + X + Y$; the shaded areas represent pseudorapidity regions of particle production.

and various theoretical models proposed to account for the breakdown of Regge factorization in SD. Our measurement severely constrains the available models, paving the way towards a more comprehensive understanding of the physics of rapidity gaps.

The components of the Collider Detector at Fermilab (CDF) most relevant to this study are the Roman pot spectrometer (RPS) [1], used to detect leading antiprotons, and the calorimeters and beam-beam counters (BBC) [12], used to detect the particles from proton-dissociation. The RPS is a forward magnetic spectrometer utilizing the accelerator magnets to measure the fractional momentum loss $\xi_{\bar{p}}$ and 4-momentum transfer squared $t_{\bar{p}}$ of the antiproton with resolutions $\delta\xi_{\bar{p}} = \pm 1.0 \times 10^{-3}$ and $\delta t_{\bar{p}} = \pm 0.07 \text{ GeV}^2$, respectively [1]. The calorimeters have projective tower geometry and cover the regions $|\eta| < 1.1$ (central), $1.1 < |\eta| < 2.4$ (plug), and $2.2 < |\eta| < 4.2$ (forward). The $\Delta\eta \times \Delta\phi$ tower dimensions are approximately $0.1 \times 15^\circ$ for the central and $0.1 \times 5^\circ$ for the plug and forward calorimeters. The BBC consist of two arrays of eight vertical and eight horizontal scintillation counters perpendicular to the beam line at $z = \pm 6 \text{ m}$, $\text{BBC}_{\bar{p}}$ and BBC_p , covering approximately the region $3.2 < |\eta| < 5.9$ in four η -segments of width $\Delta\eta \approx 0.7$.

The present study is based on our $\sqrt{s} = 1800 \text{ GeV}$ inclusive SD data sample [1]. The events were collected in the 1995-96 Tevatron Run 1C by triggering on an antiproton detected in the RPS. Offline cuts were applied requiring a reconstructed track in the RPS, no more than one reconstructed vertex in the CDF detector within a distance $|z_{\text{vtx}}| < 60 \text{ cm}$ from the nominal beam-beam interaction point along the beam direction, and a $\text{BBC}_{\bar{p}}$ multiplicity of ≤ 6 . These cuts remove overlap events due to multiple interactions in the same beam-beam crossing, comprising 4% of the inclusive SD data sample as estimated by the instantaneous luminosity.

Experimentally, since the proton side is not equipped with a RPS, we study the DPE process $\bar{p} + p \rightarrow \bar{p}' + X + Y$, where Y is either a proton or a low-mass proton-dissociation system which escapes undetected through the beam pipe; the mass squared of the system Y is estimated to be $M_Y^2 \lesssim 8 \text{ GeV}^2$. The procedure we follow to identify and measure the DPE signal in these data is to select an event sample with $(\xi_{\bar{p}}, t_{\bar{p}})$ within a certain region and measure the fractional momentum loss of the proton (or system Y) ξ_p^X using the equation [13]

$$\xi_p^X = \frac{1}{\sqrt{s}} \sum_{i=1}^n E_T^i e^{\eta^i}, \quad (1)$$

where E_T^i and η^i are the transverse energy and pseudorapidity of a particle [2] and the sum is carried out over all particles excluding the proton (or undetected particles associated with the system Y). DPE events are expected

to appear in the low ξ_p^X region, in contrast to SD events for which $\xi_p^X \approx 1$. In practice, not all particles of the system X are included in evaluating Eq. (1) because (a) CDF does not provide full coverage and (b) particles depositing energy in the calorimeters below the energy thresholds used to reject noise are excluded. This issue is addressed by applying appropriate correction factors and by calibrating formula (1) on the antiproton side by directly comparing the value of $\xi_{\bar{p}}$ obtained by this method with that measured by the RPS, $\xi_{\bar{p}}^{\text{RPS}}$, as discussed below.

To evaluate ξ_p^X we use calorimeter towers and BBC hits. The tower energy thresholds used, chosen to lie comfortably above noise level, are $E_T = 0.3 \text{ GeV}$ for the central, $E_T = 0.2 \text{ GeV}$ for the plug, and $E = 1.5 \text{ GeV}$ for the forward calorimeters; at the calorimeter interface near $|\eta| \sim 2.4$ a threshold of $E_T = 0.275 \text{ GeV}$ was used. These values are based on test-beam calibrations of the calorimeters [12] and must be multiplied by an η -dependent factor f_{E_T} (of average value $\langle f_{E_T} \rangle = 1.6$) to obtain the true E_T at low energies [14]. To account for particles below tower threshold, the calorimeter contribution to ξ_p^X is multiplied by $f_{\text{thr}} = 1.54$. This factor is obtained from a Monte Carlo (MC) simulation in which the same tower thresholds are used as in the data after dividing the generated particle energy by f_{E_T} . The Monte Carlo simulation is based on the single diffractive generator described in [8] and references therein, adapted to double-Pomeron exchange. For each BBC hit we use η and E_T values randomly chosen from a flat η distribution over the hit BBC η -segment and from the shape of the E_T distribution expected from the MC simulation, respectively. The BBC contribution to ξ_p^X is then weighted by a factor of 3/2 to account for neutral particles, which are undetected by the BBC, and by an additional factor of 3/4 to account for the overlap regions among the four scintillation counters of each BBC segment. Hits in the outer η -segments, $3.2 < |\eta| < 3.9$, which overlap with the forward calorimeters, are ignored. The BBC contribution to ξ_p^X is less than 10% in the region of $10^{-4} < \xi_p^X < 10^{-2}$ and increases to 60% at $\xi_p^X = 10^{-5}$ and $\xi_p^X = 10^{-1}$.

The method of measuring ξ using Eq. (1) is calibrated on the antiproton side by evaluating $\xi_{\bar{p}}^X \equiv \frac{1}{\sqrt{s}} \sum_{i=1}^n E_T^i e^{-\eta^i}$ (excluding the antiproton from the sum) and comparing its value with that measured by the RPS. The data are divided into bins of $\Delta\xi_{\bar{p}}^{\text{RPS}} = 0.01$, and the $\xi_{\bar{p}}^X$ values obtained for each bin are fitted with a Landau distribution. Figure 2(a) shows, as an example, the data and fit for $0.05 < \xi_{\bar{p}}^{\text{RPS}} < 0.06$. The ratio of width to peak position is ≈ 0.6 over the entire $\xi_{\bar{p}}$ region of our data sample. The enhancement in the small $\xi_{\bar{p}}^X$ region is caused by a downward shift in $\xi_{\bar{p}}^X$ in low multiplicity events due to ‘‘loss’’ of particles with energy under tower threshold. Within the region $0.01 < \xi_{\bar{p}}^{\text{RPS}} < 0.1$, an approximately linear relationship is observed between the median value of $\xi_{\bar{p}}^X$ and

$\xi_{\bar{p}}^{\text{RPS}}$. A fit with $\bar{\xi}_{\bar{p}}^X \approx C \xi_{\bar{p}}^{\text{RPS}}$ yields $C = 0.95$, in close agreement with the expected value $C = 1$. A fit in which $C \equiv 1$ and $\langle f_{E_T} \rangle$ is varied with $f_{\text{corr}} \equiv \langle f_{E_T} \rangle \times f_{\text{thr}}$ treated as a free parameter yields $f_{\text{corr}} = 2.7$. In Fig. 2(b) an error of $\pm 5\%$ is used in all data points to yield $\chi^2/\text{d.o.f.} = 1$ for this fit. In extracting results, we use $f_{\text{corr}} = 2.7$ and assign a conservative $\pm 10\%$ error to C (twice the error obtained from the fit) to account for other possible systematic uncertainties.

The DPE signal is evaluated for events with antiproton $\xi_{\bar{p}}$ and $t_{\bar{p}}$ within $0.035 < \xi_{\bar{p}} < 0.095$ and $|t_{\bar{p}}| < 1.0 \text{ GeV}^2$, where the RPS acceptance is larger than $\approx 30\%$ [1]. The total number of inclusive SD events in this region is 568 K. The calibrated $\xi_{\bar{p}}^X$ distribution is compared in Fig. 3 with a two-component MC simulation that includes SD and DPE. The shape of the input ξ_p distribution in the MC simulation for DPE is based on a triple-Pomeron term on the proton side using a Pomeron intercept $\alpha_p(0) = 1 + \epsilon$ with $\epsilon = 0.104$, as determined from a global fit to $p(\bar{p})$ total cross section data [15]. DPE events were generated for $\xi_p < 0.1$. The DPE and SD MC generated events are independently normalized to the data points in the regions $4 \times 10^{-5} < \xi_p^X < 10^{-2}$ and $0.02 < \xi_p^X < 1$, respectively. The SD events appear as a broad peak around $\xi_p^X = 1$, which falls exponentially as ξ_p^X decreases. The DPE events appear as a flattening of the distribution on the low ξ_p^X side and represent the dominant contribution for $\xi_p^X < 0.02$. The wavy shape of the data distribution in the DPE region is due to the η -dependent calorimeter tower energy thresholds used

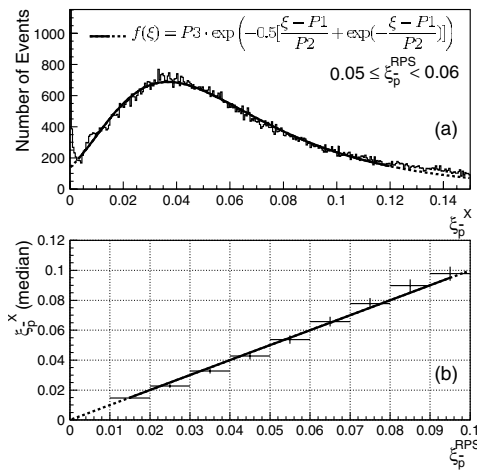


FIG. 2. (a) Distribution of antiproton fractional momentum loss $\xi_{\bar{p}}^X$ measured from calorimeter and beam-beam counter information for events in which the $\xi_{\bar{p}}^{\text{RPS}}$ value measured by the Roman pot spectrometer is within $0.05 < \xi_{\bar{p}}^{\text{RPS}} < 0.06$; the solid line is a Landau fit. (b) Median values $\bar{\xi}_{\bar{p}}^X$ obtained from Landau fits to data in different $\xi_{\bar{p}}^{\text{RPS}}$ bins plotted versus $\xi_{\bar{p}}^{\text{RPS}}$; a linear relationship is observed.

and is reproduced by the MC simulation. At low ξ_p^X both data and MC simulation extend down to and below the kinematic limit of $\xi_{p,\text{min}} = M_0^2/(s\xi_{\bar{p},\text{min}}) \approx 10^{-5}$, where M_0 is the lowest mass for DPE excitation after threshold turn-on effects set in, taken to be 1 GeV. The events below the kinematic limit are due to the downward fluctuations of ξ_p^X in low multiplicity events mentioned above. The agreement between data and MC simulation in the region of $\xi_p^X < 0.02$ shows that Regge factorization is successful in describing the shape of the ξ distribution in DPE using the Pomeron intercept determined in [15].

The ratio of the number of events within $\xi_p^X < 0.02$ to the total number of events is $0.202 \pm 0.001(\text{stat})$. After correcting for smearing effects caused by the ξ_p^X resolution, the ratio becomes $R_{\text{SD}}^{\text{DPE}} = 0.194 \pm 0.001(\text{stat}) \pm 0.012(\text{syst})$, where the systematic error is from the uncertainties due to ξ_p^X calibration (± 0.003), ξ_p^X smearing (± 0.008), and low ξ_p^X enhancement [± 0.008 , see Fig. 2(a)] added in quadrature.

Neglecting Reggeon contributions, the DPE/SD ratio is given in Regge theory by [6]

$$R_{\text{SD}}^{\text{DPE}}|_{\xi_p} = \int_{t_p=-\infty}^0 \int_{\xi_{p,\text{min}}}^{0.02} \frac{\kappa \beta^2(t_p) dt_p d\xi_p}{16\pi \xi_p^{\alpha(0)+2\alpha't_p}} \quad (2)$$

where κ is the ratio of the triple-Pomeron coupling $g(t_p)$ to the Pomeron-proton coupling $\beta(t_p)$ and $\alpha(t) = \alpha(0) + \alpha't$ is the Pomeron trajectory. Using $\kappa = 0.170 \pm 0.017$, $\beta(t_p) = \beta(0)e^{4.6t_p}$, $\beta^2(0)/16\pi = 0.86 \text{ GeV}^{-2}$, and $\alpha(t) = 1.104 + 0.25t$ [10] yields $R_{\text{SD}}^{\text{DPE}}(\text{Regge}) = 0.36 \pm 0.04$.

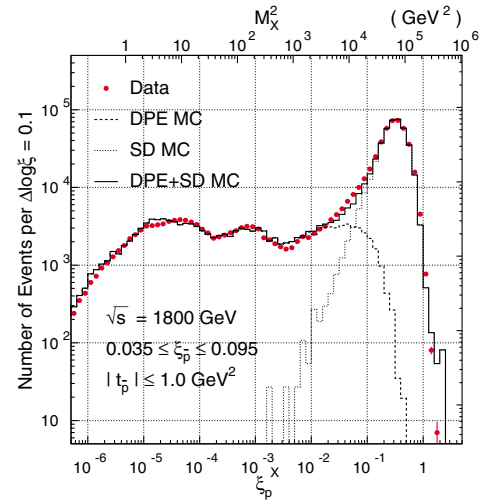


FIG. 3 (color online). Distribution of proton fractional momentum loss ξ_p^X , measured from calorimeter and beam-beam counter information, for events with a leading antiproton of $0.035 < \xi_{\bar{p}}^{\text{RPS}} < 0.095$ and $|t_{\bar{p}}| < 1.0 \text{ GeV}^2$; the curves are from a Monte Carlo simulation of SD (dotted line), DPE (dashed line) and total (solid line) contributions normalized to the data points; the DPE events were generated for $\xi_p < 0.1$.

This prediction is larger than the measured values by a factor of 1.9 ± 0.2 . However, this discrepancy from the factorization expectation of unity is small compared to the $\mathcal{O}(10)$ discrepancy observed in SD [9]. Thus, this result confirms the conjecture [6] that the formation of a rapidity gap within the rapidity space covered by the diffraction dissociation products in events with a leading (anti)proton would be largely unsuppressed. A similar conclusion has been reached by the UA8 Collaboration from a study of DPE production in $\bar{p}p$ collisions at $\sqrt{s} = 630$ GeV at the CERN $S\bar{p}pS$ collider [11]. Changes in the predicted two-gap to one-gap ratio due to contamination of the DPE signal with proton fragmentation events are estimated to be $\sim 15\%$ and therefore are not expected to alter this conclusion.

Phenomenological models proposed to account for the breakdown of Regge factorization in SD may be divided into two broadly defined classes: (a) those attributing the violation either to “damping” of the cross section at small ξ [16] or to a decrease of the Pomeron intercept at low ξ [17] or at high energies [18], and (b) those in which the overall normalization decreases with increasing energy but the shape of the ξ distribution remains practically [4,5,19] or entirely [6,9] unchanged. The models of class (a) predict a ξ_p^X distribution different from that expected from SD and are disfavored by the shape of the distribution presented in Fig. 3, which behaves as $1/\xi^{\alpha(0)}$ down to the kinematic limit of $\xi_{p,\min} \approx 10^{-5}$. Of the class (b) models, three have reported predictions for both SD and DPE: the eikonal model [19], the Pomeron flux renormalization model [9], and the gap probability renormalization model [6]. The eikonal model, in which “screening corrections” to the Regge amplitude are calculated using an eikonal approach, yields suppression factors of 0.369 and 0.309 for SD and DPE, respectively; although the DPE/SD ratio is relatively unsuppressed, in close agreement with our result, the suppression for SD is underestimated by a factor of ~ 3 . The Pomeron flux renormalization model, in which the Regge theory Pomeron flux factor is renormalized to unity for Pomerons emitted by the \bar{p} in SD or DPE and independently by the p in DPE, yields the correct suppression factor for SD, but predicts a DPE/SD ratio smaller than the measured value by a factor of 4.7 ± 0.6 [9]. Finally, in the gap probability renormalization model, in which the SD and DPE cross sections are expressed in terms of the variables M_X^2 and $\Delta\eta = \Delta\eta_{\bar{p}} + \Delta\eta_p$, where $\Delta\eta_i = -\ln\xi_i$, the predicted DPE/SD ratio is 0.21 ± 0.02 [6], in good agreement with our measured value of $0.194 \pm 0.001 \pm 0.012$. These predictions do not include possible effects from Reggeon exchange or contributions from proton fragmentation.

In summary, we have studied the double-Pomeron exchange process $\bar{p} + p \rightarrow \bar{p}' + X + Y$, where Y is a proton or a proton-dissociation system of mass squared

$M_Y^2 \lesssim 8 \text{ GeV}^2$, by measuring the fractional longitudinal momentum loss of the proton or system Y , ξ_p^X , in events with an antiproton of $0.035 < \xi_{\bar{p}} < 0.095$ and $|t_{\bar{p}}| < 1.0 \text{ GeV}^2$ produced in $\bar{p}p$ collisions at $\sqrt{s} = 1800$ GeV. Events in the region $\xi_p^X < 0.02$ follow a distribution of the form $\approx 1/\xi_p^X$ and are attributed to DPE production. The ratio of the number of DPE events in this region to the total number of events in the sample is found to be $0.194 \pm 0.001 \pm 0.012$. This value is lower than the prediction based on Regge factorization by a factor of 1.9 ± 0.2 , which is relatively small compared to the suppression factor of $\mathcal{O}(10)$ observed in SD [9], indicating that the formation of a second rapidity gap in a SD event is relatively unsuppressed. Among models proposed to explain the suppression of the SD cross section at high energies, our results favor those in which the Regge based shapes of the SD and DPE distributions remain unchanged and only the overall normalization is suppressed [4–6,9,19].

We thank the Fermilab staff and the technical staffs of the participating institutions for their vital contributions. This work was supported by the U.S. Department of Energy and National Science Foundation; the Italian Istituto Nazionale di Fisica Nucleare; the Ministry of Education, Culture, Sports, Science and Technology of Japan; the Natural Sciences and Engineering Research Council of Canada; the National Science Council of the Republic of China; the Swiss National Science Foundation; the A. P. Sloan Foundation; the Bundesministerium fuer Bildung und Forschung, Germany; and the Korea Science and Engineering Foundation.

-
- [1] CDF Collaboration, T. Affolder *et al.*, Phys. Rev. Lett. **84**, 5043 (2000).
 - [2] The pseudorapidity and transverse energy of a particle of energy E and polar angle θ (measured from the proton beam direction) are defined as $\eta = -\ln(\tan\frac{\theta}{2})$ and $E_T = E \sin\theta$, respectively.
 - [3] V. Barone and E. Predazzi, *High-Energy Particle Diffraction*, (Springer Press, New York, 2001).
 - [4] See, for example, E. Gotsman, E. M. Levin, and U. Maor, Phys. Rev. D **60**, 094011 (1999).
 - [5] A. B. Kaidalov, V. A. Khoze, A. D. Martin, and M. G. Ryskin, Eur. Phys. J. C **21**, 521 (2001).
 - [6] K. Goulios, hep-ph/0110240; hep-ph/0203141.
 - [7] CDF Collaboration, T. Affolder *et al.*, Phys. Rev. Lett. **87**, 141802 (2001).
 - [8] CDF Collaboration, F. Abe *et al.*, Phys. Rev. D **50**, 5535 (1994).
 - [9] K. Goulios, Phys. Lett. B **358**, 379 (1995); **363**, 268 (1995).
 - [10] K. Goulios and J. Montanha, Phys. Rev. D **59**, 114017 (1999).

- [11] UA8 Collaboration, A. Brandt *et al.*, Eur. Phys. J. C **25**, 361 (2002).
- [12] CDF Collaboration, F. Abe *et al.*, Nucl. Instrum. Methods Phys. Res., Sect. A **271**, 387 (1988).
- [13] J. Collins, hep-ph/9705393.
- [14] S. Bagdasarov, PhD thesis, Rockefeller University, (1997).
- [15] R.J.M. Covolan, J. Montanha and K. Goulianos, Phys. Lett. B **389**, 176 (1996).
- [16] S. Erhan and P. Schlein, Phys. Lett. B **427**, 389 (1998).
- [17] Chung-I Tan, Phys. Rep. **315**, 175 (1999).
- [18] S. Erhan and P. Schlein, Phys. Lett. B **481**, 177 (2000).
- [19] E. Gotsman, E.M. Levin, and U. Maor, Phys. Lett. B **353**, 526 (1995).